

## **SUPPLEMENTAL MATERIAL**

### **Supplemental Methods**

#### **Cell cultures**

HUVECs, bovine aortic ECs (BAECs), and human embryonic kidney 293 (HEK293) cells were cultured by standard methods<sup>1</sup>.

#### **Plasmid construction and luciferase assay**

The Luc-KLF2 reporter was constructed by inserting the full-length human KLF2 3'UTR into pMIR-REPORT vector (Ambion). The FLAG-KLF2 plasmid was constructed by fused a CMV-driven FLAG tag with KLF2 cDNA (including 3'UTR). Luc-KLF2 (Luc-mut) and FLAG-KLF2(mut) with a mutated miR-92a binding site were created by using QuickChange site-directed mutagenesis (Stratagene, La Jolla, CA). The deletion of the miR-92a binding site in FLAG-KLF2( $\Delta$ ) was constructed by two-step PCR<sup>2</sup>. The miR-92a reporter (Luc-92a) contained a luciferase reporter and 2 copies of sequences complementary to miR-92a (Luc-2xmiR92a). The reporter constructs were co-transfected with pre-92a or anti-92a (20 nM) into HEK293 cells or BAECs by use of lipofectamine 2000 (Invitrogen). Luciferase expression was measured by luciferase reporter and  $\beta$ -galactosidase enzyme assays (Promega, Madison, WI).

## **Computational analysis for KLF2-regulated miRNAs**

The transcriptional start sites (TSSs) of the selected miRNAs were obtained from miRStart database (<http://mirstart.mbc.nctu.edu.tw/>), which contains the predicted promoters of human miRNAs. The miRNA promoters were identified by the supports of several experimental datasets derived from TSS-relevant experiments, including CAGE tags, TSS Seq tags and CHIP-seq of H3K4me3 enrichment.

JASPAR<sup>3</sup> was utilized to identify the potential binding sites of KLF2 within the promoter regions (flanking -3000~+500 according to TSS) of the reported shear-regulated miRNAs. The position weighted matrix (PWM) of KLF4 was used to identify KLF2-regulated miRNAs since the binding motifs of KLF2 and KLF4 are highly similar.

## **Immunoprecipitation (IP)-miR-induced silencing complex (miRISC)**

HUVECs were harvested with the lysis buffer containing 50 mM Tris, pH 7.5, 150 mM NaCl, 0.1% NP-40, 1 mM EDTA, and 100 units/ $\mu$ l RNase inhibitor. The lysates were incubated with anti-Ago1 or Ago2 antibody (2  $\mu$ g/mg protein) (Cell Signaling) at 4°C overnight and then protein A agarose beads (25  $\mu$ l beads per ml) for 4 hr. The beads were then spun down and the immunoprecipitated RNAs were extracted with Trizol reagent (Invitrogen).

## **NO bioavailability assay**

The NO production from cells was detected as the accumulated nitrite/nitrate, the

stable breakdown product of NO, in cell culture media by using nitrate/nitrite fluorometric assay (Cayman Chemicals, Ann Arbor, MI). HUVECs were transfected with pre-92a or control RNA and infected with Ad-KLF2 or Ad-GFP for 48 hr. The DMEM in the absence of FBS and phenol red was then substituted and incubated further for 16 hr. The conditioned medium was filtered through a 10 KD MW cut-off filter (Millipore) to remove ingredients that caused an interference of the fluorescence intensity. Nitrate was first reduced to nitrite by nitrate reductase, and then the total nitrite concentration was determined by forming the fluorescent product with 2,3-Diaminonaphthalene (DAN). The fluorescent readings were obtained using SpectraMax M5 Multi-Detection Reader (BD Biosciences, Palo Alto, CA) with excitation at 360 nm and emission at 430 nm. The readings were normalized to the total cell number. The NO<sub>x</sub> concentrations were then calculated according to an established calibration curve.

### **Flow-induced vasodilation**

The animal experimental protocols were approved by the Institutional Animal Care and Use Committee of University of California, Riverside. F-127 pluronic gel (Sigma) was used to deliver pre-92a into the carotid artery of 7- to 10-week old male C57BL6 mice<sup>4</sup>. Five days after the local oligo delivery, animals were killed and the pluronic gel-coated vessels were isolated. For the flow-induced vasodilation, the isolated mouse carotid arteries were mounted on 2 glass cannulae in a perfusion myograph chamber connected to the SoftEdge

Acquisition Subsystem (Living Systems, Burlington, VT). The vessel chamber was perfused with warmed physiological salt solution containing 130 mM NaCl, 10 mM HEPES, 6 mM glucose, 4 mM KCl, 4 mM NaHCO<sub>3</sub>, 1.8 mM CaCl<sub>2</sub>, 1.18 mM KH<sub>2</sub>PO<sub>4</sub>, 1.2 mM MgSO<sub>4</sub>, and 0.025 mM EDTA, pH 7.4. Images of carotid arteries were obtained by a video camera attached to a Nikon TS100 inverted microscope. A video dimension analyzer (Living System) was used to measure the external diameter of arteries, and data were collected by use of BioPac MP100 hardware and Biopac AcqKnowledge software (BioPac, Goleta, CA). The arteries were maintained at an intraluminal pressure of 100 mmHg for the duration of the experiment, then equilibrated for 30 min before extraluminal administration of 1 μM phenylephrine (Sigma). After maximal constriction, flow rate was increased to 400 μl/min, which corresponds to the physiological range in mouse carotid arteries<sup>5</sup>. L-NAME (1 mM), acetylcholine (1 μM), and sodium nitroprusside (SNP) (1 μM) was applied. The vessel diameter changes induced by flow were then recorded.

**Supplemental Table 1: Flow-induced dilation of carotid arteries**

	Treatment	n*	Diameter ( $\mu\text{m}$ )	
			Control RNA	Pre-92a
<b>Control</b>	Initial	9	306.0 $\pm$ 7.1	298.3 $\pm$ 6.9
	Constricted	9	274.3 $\pm$ 7.6	251.9 $\pm$ 9.9
	$\Delta$ constriction <sup>†</sup>	9	30.7 $\pm$ 5.4	46.4 $\pm$ 11.1
	Post-flow	9	285.9 $\pm$ 8.6	257.1 $\pm$ 9.3
	$\Delta$ dilation <sup>†</sup>	9	11.6 $\pm$ 2.2	5.2 $\pm$ 1.6
	Dilation ability <sup>‡</sup>	9	43.7% $\pm$ 9.3%	11.9% $\pm$ 3.0% <sup>§</sup>
<b>L-NAME</b>	Initial	5	298.0 $\pm$ 9.1	299.0 $\pm$ 9.5
	Constricted	5	243.8 $\pm$ 8.4	238.8 $\pm$ 8.5
	$\Delta$ constriction <sup>†</sup>	5	34.8 $\pm$ 5.0	38.4 $\pm$ 12.4
	Post-flow	5	250.4 $\pm$ 6.5	243.2 $\pm$ 7.6
	$\Delta$ dilation <sup>†</sup>	5	6.8 $\pm$ 2.2	5.4 $\pm$ 2.0
	Dilation ability <sup>‡</sup>	5	18.1% $\pm$ 5.5% <sup>§</sup>	15.6% $\pm$ 5.4%
<b>Ach</b>	Constricted	5	274.4 $\pm$ 7.8	264.7 $\pm$ 7.0
	Ach	5	289.1 $\pm$ 8.6	263.0 $\pm$ 9.6
	$\Delta$ dilation <sup>†</sup>	5	14.7 $\pm$ 1.8	-1.7 $\pm$ 6.5
<b>SNP</b>	Constricted	5	254.9 $\pm$ 9.0	252.0 $\pm$ 6.7
	SNP	5	294.7 $\pm$ 7.0	298.9 $\pm$ 7.5
	$\Delta$ dilation <sup>†</sup>	5	40.0 $\pm$ 6.0	46.7 $\pm$ 5.9

\* n denotes the number of animals

<sup>†</sup>  $\Delta$ : the diameter changes of the carotid arteries after the treatment.

<sup>‡</sup> Dilation ability: the diameter change of the flow-induced dilation compared to the diameter change of the PE-induced constriction.

<sup>§</sup>  $p < 0.05$  pre-92a treated group vs. corresponding control group; L-NAME treated group vs.

non-treated control group.

Data are presented as mean $\pm$ SEM.

**Supplemental Table 2. Transcription factors regulating KLF2**

<b>TF</b>	<b>Regulation mode</b>	<b>Shear regulated</b>	<b>References</b>
MEF2A	Activated	yes	6-8
MEF2C	Activated	yes	6-8
BRG1	Unspecified	unknown	9
p300	Activated	yes	10-13
PCAF	Activated	Yes	11,13
hnRNP D	Activated	Yes	11,13
hnRNP U	Activated	Yes	11,13
Nucleolin	Activated	Yes	14
SP1	Activated	yes	15
Oct-3/4	Activated	unknown	16-19
SOX2	Activated	unknown	16,17,20

**Supplemental Table 3. Transcription factors regulating the miR-17~92 cluster**

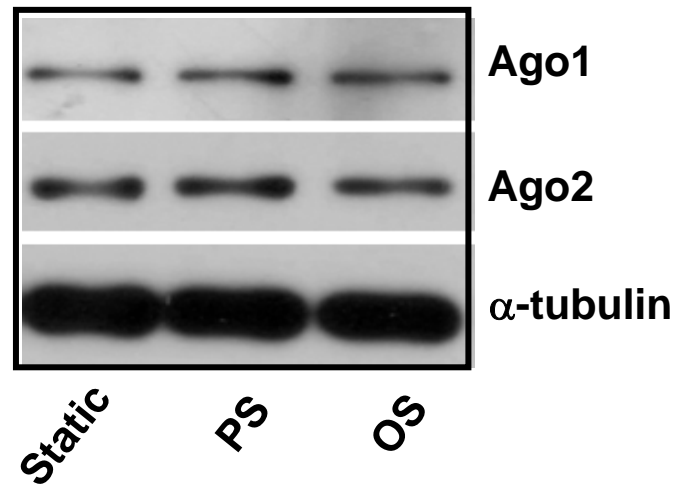
<b>TF</b>	<b>Regulation mode</b>	<b>Shear inducible</b>	<b>References</b>
c-Myc	Activated	Inhibited	21,22
E2F	Activated	Inhibited	23,24
STAT3	Activated	Inhibited	25,26
cyclin D1	Activated	Inhibited	27
P53	Inhibited	Activated	28,29
RUNX1	Inhibited	Inhibited	30
ATF2	Predicted	Inhibited	31
CREB	Predicted	Activated	32
PPARG	Predicted	Inhibited	33
SP1	Predicted	Activated	34

**Supplemental Table 4. KLF2-targeted miRNAs**

<b>Gene</b>	<b>Host gene</b>	<b>function</b>	<b>Validated</b>	<b>Reference</b>
hsa-miR-126	Egfl7	Angiogenesis Anti-inflammation	Yes	35,36
hsa-miR-30a	C6orf155	angiogenesis	predicted	36-38
hsa-miR-483-5p	IGF2	metabolism	predicted	39
hsa-miR-101-1	Intergenic	Cell growth	predicted	37,40
hsa-miR-181d	Intergenic	differentiation	predicted	37,41
hsa-miR-15a	DLEU2	apoptosis	predicted	37,42
hsa-miR-148a	Intergenic	Cell survival	predicted	37,43
hsa-miR-365-1	Intergenic	unknown	predicted	37

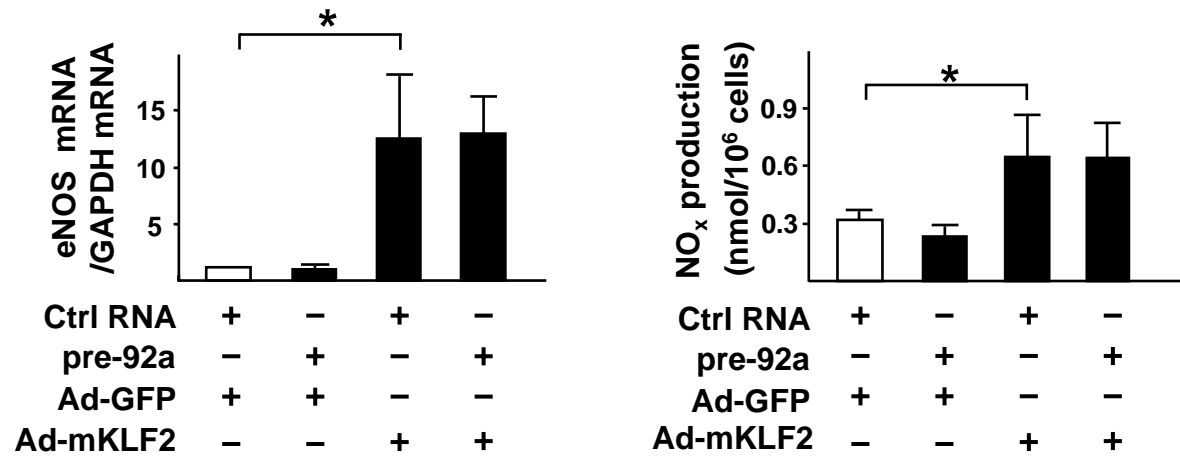


## Supple Fig. 1



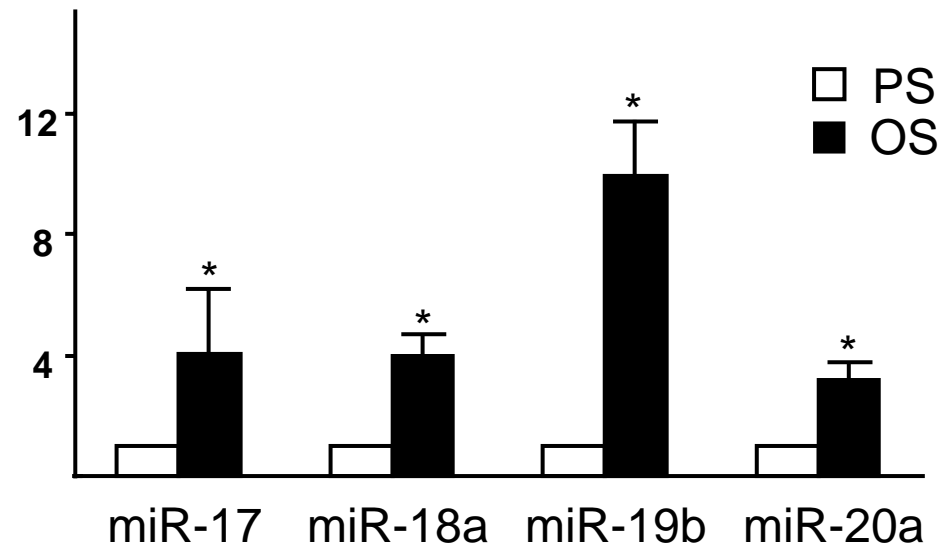
**Supple Fig. 1.** HUVECs were exposed to a PS ( $12 \pm 4$  dyn/cm<sup>2</sup>) or OS ( $0 \pm 4$  dyn/cm<sup>2</sup>) for 8 hr and then lysed. Protein levels of Ago1 and Ago2 assessed by Western blot analysis with anti-Ago1 and anti-Ago2 and normalized to that of  $\alpha$ -tubulin.

## Suppl. Fig. 2



**Supple Fig. 2.** HUVECs were transfected with pre-92a (20 nM) and infected with Ad-mKLF2 (without 3'UTR) (ref. 44) or Ad-GFP (10 MOI) for 48 hr. The level of eNOS mRNA was assessed by qRT-PCR and the released NO<sub>x</sub> was measured by nitrate/nitrite fluorometric assay.

### Supple Fig. 3



**Supple Fig. 3.** HUVECs were exposed to a PS ( $12 \pm 4$  dyn/cm<sup>2</sup>) or OS ( $0 \pm 4$  dyn/cm<sup>2</sup>) for 24 hr and then lysed. The amount of miRNAs were assessed by miRNA microarray. The level of ECs exposed to OS, averaged from 3 experiments was normalized to that of cells exposed to PS.

## Reference

1. Gimbrone MA, Jr., Cotran RS, Folkman J. Human vascular endothelial cells in culture. Growth and DNA synthesis. *J Cell Biol.* 1974; 60:673-684.
2. Ogel ZB, McPherson MJ. Efficient deletion mutagenesis by PCR. *Protein Eng.* 1992; 5:467-468.
3. Bryne JC, Valen E, Tang MH, Marstrand T, Winther O, da Piedade I, Krogh A, Lenhard B, Sandelin A. JASPAR, the open access database of transcription factor-binding profiles: new content and tools in the 2008 update. *Nucleic Acids Res.* 2008; 36(Database issue):D102-106.
4. Forte A, Galderisi U, De Feo M, Gomez MF, Esposito S, Sante P, Renzulli A, Agozzino L, Hellstrand P, Berrino L, Cipollaro M, Cotrufo M, Rossi F, Cascino A. c-Myc antisense oligonucleotides preserve smooth muscle differentiation and reduce negative remodelling following rat carotid arteriotomy. *J Vasc Res.* 2005; 42:214-225.
5. Eitzman DT, Bodary PF, Shen Y, Khairallah CG, Wild SR, Abe A, Shaffer-Hartman J, Shayman JA. Fabry disease in mice is associated with age-dependent susceptibility to vascular thrombosis. *J Am Soc Nephrol.* 2003; 14:298-302.
6. Sako K, Fukuhara S, Minami T, Hamakubo T, Song H, Kodama T, Fukamizu A, Gutkind JS, Koh GY, Mochizuki N. Angiopoietin-1 induces Kruppel-like factor 2 expression through a phosphoinositide 3-kinase/AKT-dependent activation of myocyte

- enhancer factor 2. *J Biol Chem.* 2009; 284:5592-5601.
7. Kumar A, Lin Z, SenBanerjee S, Jain MK. Tumor necrosis factor alpha-mediated reduction of KLF2 is due to inhibition of MEF2 by NF-kappaB and histone deacetylases. *Mol Cell Biol.* 2005; 25:5893-5903.
  8. Parmar KM, Larman HB, Dai G, Zhang Y, Wang ET, Moorthy SN, Kratz JR, Lin Z, Jain MK, Gimbrone MA, Jr., Garcia-Cardena G. Integration of flow-dependent endothelial phenotypes by Kruppel-like factor 2. *J Clin Invest.* 2006; 116:49-58.
  9. Kidder BL, Palmer S, Knott JG. SWI/SNF-Brg1 regulates self-renewal and occupies core pluripotency-related genes in embryonic stem cells. *Stem Cells.* 2009; 27:317-328.
  10. SenBanerjee S, Lin Z, Atkins GB, Greif DM, Rao RM, Kumar A, Feinberg MW, Chen Z, Simon DI, Luscinskas FW, Michel TM, Gimbrone MA, Jr., Garcia-Cardena G, Jain MK. KLF2 Is a novel transcriptional regulator of endothelial proinflammatory activation. *J Exp Med.* 2004; 199:1305-1315.
  11. Ahmad N, Lingrel JB. Kruppel-like factor 2 transcriptional regulation involves heterogeneous nuclear ribonucleoproteins and acetyltransferases. *Biochemistry.* 2005; 44:6276-6285.
  12. Chen W, Bacanamwo M, Harrison DG. Activation of p300 histone acetyltransferase activity is an early endothelial response to laminar shear stress and is essential for stimulation of endothelial nitric-oxide synthase mRNA transcription. *J Biol Chem.* 2008;

283:16293-16298.

13. Huddleson JP, Ahmad N, Srinivasan S, Lingrel JB. Induction of KLF2 by fluid shear stress requires a novel promoter element activated by a phosphatidylinositol 3-kinase-dependent chromatin-remodeling pathway. *J Biol Chem.* 2005; 280:23371-23379.
14. Huddleson JP, Ahmad N, Lingrel JB. Up-regulation of the KLF2 transcription factor by fluid shear stress requires nucleolin. *J Biol Chem.* 2006; 281:15121-15128.
15. Schrick JJ, Hughes MJ, Anderson KP, Croyle ML, Lingrel JB. Characterization of the lung Kruppel-like transcription factor gene and upstream regulatory elements. *Gene.* 1999; 236:185-195.
16. Liu X, Huang J, Chen T, Wang Y, Xin S, Li J, Pei G, Kang J. Yamanaka factors critically regulate the developmental signaling network in mouse embryonic stem cells. *Cell Res.* 2008; 18:1177-1189.
17. Sharov AA, Masui S, Sharova LV, Piao Y, Aiba K, Matoba R, Xin L, Niwa H, Ko MS. Identification of Pou5f1, Sox2, and Nanog downstream target genes with statistical confidence by applying a novel algorithm to time course microarray and genome-wide chromatin immunoprecipitation data. *BMC Genomics.* 2008; 9:269.
18. Sridharan R, Tchieu J, Mason MJ, Yachechko R, Kuoy E, Horvath S, Zhou Q, Plath K. Role of the murine reprogramming factors in the induction of pluripotency. *Cell.* 2009;

136:364-377.

19. Bruce SJ, Gardiner BB, Burke LJ, Gongora MM, Grimmond SM, Perkins AC. Dynamic transcription programs during ES cell differentiation towards mesoderm in serum versus serum-freeBMP4 culture. *BMC Genomics*. 2007; 8:365.
20. Kim J, Chu J, Shen X, Wang J, Orkin SH. An extended transcriptional network for pluripotency of embryonic stem cells. *Cell*. 2008; 132:1049-1061.
21. O'Donnell KA, Wentzel EA, Zeller KI, Dang CV, Mendell JT. c-Myc-regulated microRNAs modulate E2F1 expression. *Nature*. 2005; 435:839-843.
22. Magid R, Murphy TJ, Galis ZS. Expression of matrix metalloproteinase-9 in endothelial cells is differentially regulated by shear stress. Role of c-Myc. *J Biol Chem*. 2003; 278:32994-32999.
23. Sylvestre Y, De Guire V, Querido E, Mukhopadhyay UK, Bourdeau V, Major F, Ferbeyre G, Chartrand P. An E2F/miR-20a autoregulatory feedback loop. *J Biol Chem*. 2007; 282:2135-2143.
24. Akimoto S, Mitsumata M, Sasaguri T, Yoshida Y. Laminar shear stress inhibits vascular endothelial cell proliferation by inducing cyclin-dependent kinase inhibitor p21(Sdi1/Cip1/Waf1). *Circ Res*. 2000; 86:185-190.
25. Brock M, Trenkmann M, Gay RE, Michel BA, Gay S, Fischler M, Ulrich S, Speich R, Huber LC. Interleukin-6 modulates the expression of the bone morphogenic protein

- receptor type II through a novel STAT3-microRNA cluster 17/92 pathway. *Circ Res.* 2009; 104:1184-1191.
26. Ni CW, Hsieh HJ, Chao YJ, Wang DL. Interleukin-6-induced JAK2/STAT3 signaling pathway in endothelial cells is suppressed by hemodynamic flow. *Am J Physiol Cell Physiol.* 2004; 287:C771-780.
27. Yu Z, Wang C, Wang M, Li Z, Casimiro MC, Liu M, Wu K, Whittle J, Ju X, Hyslop T, McCue P, Pestell RG. A cyclin D1/microRNA 17/20 regulatory feedback loop in control of breast cancer cell proliferation. *J Cell Biol.* 2008; 182:509-517.
28. Yan HL, Xue G, Mei Q, Wang YZ, Ding FX, Liu MF, Lu MH, Tang Y, Yu HY, Sun SH. Repression of the miR-17-92 cluster by p53 has an important function in hypoxia-induced apoptosis. *EMBO J.* 2009; 28:2719-2732.
29. Lin K, Hsu PP, Chen BP, Yuan S, Usami S, Shyy JY, Li YS, Chien S. Molecular mechanism of endothelial growth arrest by laminar shear stress. *Proc Natl Acad Sci U S A.* 2000; 97:9385-9389.
30. Fontana L, Pelosi E, Greco P, Racanicchi S, Testa U, Liuzzi F, Croce CM, Brunetti E, Grignani F, Peschle C. MicroRNAs 17-5p-20a-106a control monocytopoiesis through AML1 targeting and M-CSF receptor upregulation. *Nat Cell Biol.* 2007; 9:775-787.
31. Fledderus JO, van Thienen JV, Boon RA, Dekker RJ, Rohlena J, Volger OL, Bijmens AP, Daemen MJ, Kuiper J, van Berkel TJ, Pannekoek H, Horrevoets AJ. Prolonged shear



- stress and KLF2 suppress constitutive proinflammatory transcription through inhibition of ATF2. *Blood*. 2007; 109:4249-4257.
- 32.** Boo YC. Shear stress stimulates phosphorylation of protein kinase A substrate proteins including endothelial nitric oxide synthase in endothelial cells. *Exp Mol Med*. 2006; 38:453.
- 33.** Braam B, de Roos R, Bluysen H, Kemmeren P, Holstege F, Joles JA, Koomans H. Nitric oxide-dependent and nitric oxide-independent transcriptional responses to high shear stress in endothelial cells. *Hypertension*. 2005; 45:672-680.
- 34.** Yun S, Dardik A, Haga M, Yamashita A, Yamaguchi S, Koh Y, Madri JA, Sumpio BE. Transcription factor Sp1 phosphorylation induced by shear stress inhibits membrane type 1-matrix metalloproteinase expression in endothelium. *J Biol Chem*. 2002; 277:34808-34814.
- 35.** Harris TA, Yamakuchi M, Kondo M, Oettgen P, Lowenstein CJ. Ets-1 and Ets-2 Regulate the Expression of MicroRNA-126 in Endothelial Cells. *Arterioscler Thromb Vasc Biol*. 2010; 30:1990-1997.
- 36.** Weber M, Baker MB, Moore JP, Searles CD. MiR-21 is induced in endothelial cells by shear stress and modulates apoptosis and eNOS activity. *Biochem Biophys Res Commun*. 2010; 393:643-648.
- 37.** Qin X, Wang X, Wang Y, Tang Z, Cui Q, Xi J, Li YS, Chien S, Wang N.

- MicroRNA-19a mediates the suppressive effect of laminar flow on cyclin D1 expression in human umbilical vein endothelial cells. *Proc Natl Acad Sci U S A*. 2010; 107:3240-3244.
- 38.** Wang KC, Garmire LX, Young A, Nguyen P, Trinh A, Subramaniam S, Wang N, Shyy JY, Li YS, Chien S. Role of microRNA-23b in flow-regulation of Rb phosphorylation and endothelial cell growth. *Proc Natl Acad Sci U S A*. 2010; 107:3234-3239.
- 39.** Mellick AS, Plummer PN, Nolan DJ, Gao D, Bambino K, Hahn M, Catena R, Turner V, McDonnell K, Benezra R, Brink R, Swarbrick A, Mittal V. Using the transcription factor inhibitor of DNA binding 1 to selectively target endothelial progenitor cells offers novel strategies to inhibit tumor angiogenesis and growth. *Cancer Res*. 2010; 70:7273-7282.
- 40.** Strillacci A, Griffoni C, Sansone P, Paterini P, Piazzzi G, Lazzarini G, Spisni E, Pantaleo MA, Biasco G, Tomasi V. MiR-101 downregulation is involved in cyclooxygenase-2 overexpression in human colon cancer cells. *Exp Cell Res*. 2009; 315:1439-1447.
- 41.** Kazenwadel J, Michael MZ, Harvey NL. Prox1 expression is negatively regulated by miR-181 in endothelial cells. *Blood*. 2010; 116:2395-2401.
- 42.** Yin KJ, Deng Z, Hamblin M, Xiang Y, Huang H, Zhang J, Jiang X, Wang Y, Chen YE. Peroxisome proliferator-activated receptor delta regulation of miR-15a in ischemia-induced cerebral vascular endothelial injury. *J Neurosci*. 2010; 30:6398-6408.

43. Wagner-Ecker M, Schwager C, Wirkner U, Abdollahi A, Huber PE. MicroRNA expression after ionizing radiation in human endothelial cells. *Radiat Oncol.* 2010; 5:25.
  
44. SenBanerjee S, Lin Z, Atkins GB, Greif DM, Rao RM, Kumar A, Feinberg MW, Chen Z, Simon DI, Luscinskas FW, Michel TM, Gimbrone MA, Jr., Garcia-Cardena G, Jain MK. KLF2 Is a novel transcriptional regulator of endothelial proinflammatory activation. *J Exp Med.* 2004; 199:1305-1315.